Universiteit Utrecht

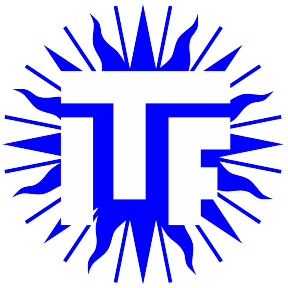

Faculteit Bètawetenschappen

Multimode Effects on a Bose-Einstein Condensate of photons in a Dye-Filled Microcavity

Bachelor Thesis

C.B. Marinissen

Mathematics & Physics
TWIN

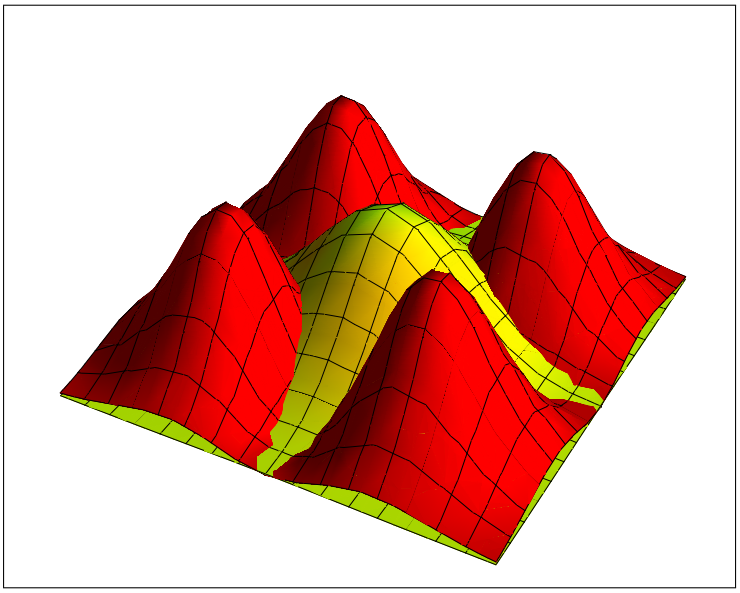

Supervisor:

Prof. H.T.C. Stoof
Institute for Theoretical Physics

June 2018

Abstract

In this bachelor's thesis we study multi-mode effects on the Bose-Einstein condensation (BEC) of photons in a dye-filled microcavity. The repulsive effective interaction of the photons should increase the condensate size. We show how the condensate radius of the ground state and an excited state depend on this effective interaction of the photons. We show that the spatial form of the excited state can also decrease the radius of the ground state. For this effect to occur, we expect a sufficiently large effective interaction. Comparing our model with experimental data gives us an effective interaction of $\tilde{g} = (5.2 \pm 2.3) \times 10^{-5}$. However, one should interpret this result with care, because better measurements of the photon occupation numbers are needed before we can reach solid conclusions.

We further investigate rate equations for the BEC of photons to understand the stationary photon occupation numbers. We find approximated solutions to these rate equations to find the dependence of the photon occupation numbers on the pump rate which excites the dye molecules in the condensate. Despite those approximations we estimate critical parameters for which either lasing or saturation of the photon numbers is expected. We conclude that the rate of decay from the cavity and emission rates of the dye is very important. From comparing the model with experiment we can conclude that the approximations are well enough to capture the right trend of real data. However, in the limit of large photon numbers, the approximations aren't good enough anymore and a more accurate approach will be necessary.

Contents

1 Introduction

With the introduction of quantum mechanics in the 20^{th} century, a whole new area of physics was discovered. Within this new area, a lot of rules were discovered, different from the known rules of classical mechanics. To find out whether we need to apply the concepts of quantum mechanics Louis de Broglie found a simple hypothesis. In his rule, he states that a particle has wave-like behavior when the average interparticle distance is smaller than de Broglie wavelength

$$\lambda = \frac{\hbar}{\sqrt{2mk_BT}}, \tag{1}$$

with $\hbar$ the reduced Planck's constant, m the mass of the particle, k_B Boltzmann's constant and T the temperature of the system. One of the cases when this happens is a Bose-Einstein condensate (BEC). In this state, the de Broglie wavelength of the particles is so large that they overlap and the particles aren't distinguishable. BEC was first predicted by A. Einstein [1] and can roughly be defined as the macroscopic occupation of the ground state at thermal equilibrium. In the recent years BEC's have been formed using ultra-cold atomic Bose gases and it is the ideal playground to study macroscopic quantum systems.

1.1 Bose-Einstein condensate of photons

One would expect that the ideal photon gas, associated with blackbody radiation, would show Bose-Einstein condensation. Photons can indeed be brought into thermal equilibrium in a black box, but at low temperatures photons disappear in the cavity walls which implies that the chemical potential is strictly zero. A macroscopic occupation of the cavity ground state will therefore not occur. It was not until 2010 before a Bose-Einstein condensate of photons was realized by using a dye-filled optical microcavity [2]. Since then, interest in this kind of BEC has grown, because of its relatively simple set up. Since 2010, three research groups have realized a photon BEC [2–4] and the literature on the subject has grown extensively [5].

1.2 Photon-photon interactions

Recent work on the subject focused on the effective interactions for the BEC of photons. The nature of the interaction isn't clear yet, so different results for the interaction have been found. Klaers et al. [6] where the first that claimed to have found an interaction between the photons. For a noninteracting ideal photon gas, one expects that the condensate size remains the same. However, Klaers et al. [6] measured that the condensate radius enlarges with an increasing condensate fraction. They explained this by assuming a repulsive interaction between the photons. Using a theoretical model, based on the Gross-Pitaevskii equation, they estimate the dimensionless interaction parameter to be $\tilde{g} = (7 \pm 3) \times 10^{-4}$.

Other research groups have also studied the effective interaction. Marelic et al. [7] used a model based on the quasi-particle dispersion in the condensate and found $\tilde{g} = 10^{-4}$. They even determined an upper limit of $\tilde{g} \leq 10^{-3}$.

Greveling et al. [4] also looked at the condensate radius and condensate photon number. They even did this for several dye concentrations from which they concluded that the effective interaction strength decreases with increasing dye concentration. Their effective interaction, for all dye concentrations, is of the order $\tilde{g} \simeq 10^{-2}$. However, this is more then one order of magnitude larger then what the other groups estimated.

Besides the experimental determinations of the effective interaction, van der Wurff et al. [8] even tried to find possible mechanisms for the photon-photon interaction. However, these different theoretical models yield interaction strengths $10^{-9} \leq \tilde{g} \leq 10^{-4}$, which is typically much lower then these of the experimental research groups.

1.3 Research question

Inspired by the work of Greveling et al. [4], which determined a much larger effective interaction then the other research groups, we want to make a model for the effective interaction as well. The reason that their effective interaction is likely too large is due to the fact that theoretically only the ground state of the photons is taken into account, while excited states contribute to the experimental measured condensate size as well. With this in mind we want to improve the description and add the effects of an excited state. This leaves us with the main research question of this thesis:

- What is the effective photon-photon interaction strength in a Bose-Einstein Condensate of photons when looking at the condensate radius for the ground state interacting with an excited state?

So the goal of this bachelor's research is to add the contribution of an excited state. While we derived this model we had good contact with the research group of Dries van Oosten, which determined the effective interaction of Greveling et al. [4]. They provided us with the necessary insight in the experiment and with data to compare our theoretical models with.

As this bachelor's research proceeded, we encountered certain limits of our theoretical model. We were able to get the effective interaction from the condensate radius of the ground state and the excited state. However, we weren't able to explain the photon occupation numbers of the different states. We found out which phenomena need to be taken into account to describe these photon numbers. One of this phenomena is a pump laser which is necessary to realize a BEC of photons. With this insight, we came up with the extra research question:

- What describes the photon occupation numbers of different states in the BEC of photons and how does it depend on the pump laser?

1.4 Outline

This thesis can be devided into two different parts. On the one hand, we discuss the effective interaction and compare this to earlier results. On the other hand, we want to say something about the photon occupation numbers. The precise layout of the thesis is as follows.

In section 2 we look at some prerequisites. Before we can answer our research question we must understand the experimental set up. From this, the characteristic equations for a photon BEC follow (section 2.2 and 2.3) and we will find out that the photons behave like massive particles in a two-dimensional harmonic trap. This can be used later on. At the end of this section, we discuss the results of Greveling et al. [4] for the effective interaction. As we have said before, we will argue that this estimate of the effective interaction is too large and this will be the main motivation for this bachelor's research.

After we have determined the characteristic equations for a photon BEC, we identify in section 3.1 similar equations as in Greveling et al. [4] to describe the effective interaction. However, we solve these equations with a variational ansatz for both sizes of the ground state and an excited state. Our variational parameters are a direct measure for the condensate radius of these states. Using perturbation theory, we find in section 3.3 solutions for our variational parameters. At the end of this section we will discuss these results and compare them to the results of Greveling et al. [4]. Furthermore we identify certain limits of our model. This is the motivation for the next section.

In section 4 we first try to understand the physical phenomena of the BEC of photons including the pump laser. From this, the equations to describe the photon numbers and the excitation density of the dye, follow in section 4.2. Because these equations can't be solved analytical, we try to find approximated solutions for the equilibrium situation. In section 4.5 we will discuss our results by looking at different limits.

To conclude we compare in section 5 our models with experimental data, provided by the research group of Dries van Oosten. We apply our models to find an effective interaction. We furthermore see that our models for the photon occupation numbers capture the right trend and they show that the decay rate from the cavity is an important parameter in the experiment.

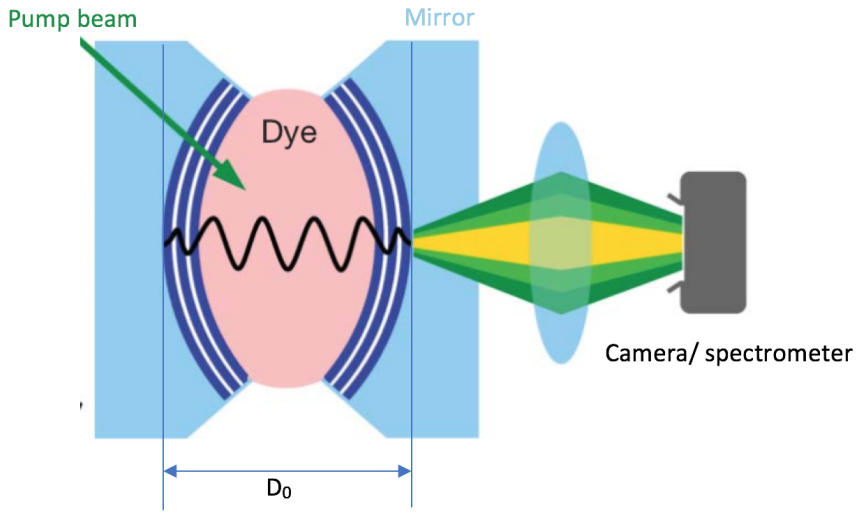

Figure 1: Schematic picture of the experimental set-up of the Bose-Einstein condensate of photons [6]

2 Prerequisites

In this section we discuss a few concepts of a Bose-Einstein condensate of photons. These will be of great use in the following sections of this thesis. First of all, we need to understand the experimental set up. From this, we can identify the dispersion relation of the photons in the condensate. We find that the photons behave like massive particles in a harmonic potential. At the end of this section, we discuss the effective interaction as determined by Greveling et al. [4] and argue why this is an overestimation. This is the main motivation for the next section.

2.1 Experimental set-up

In 2010 Klaers et al. [2] were the first to realize a BEC of photons. They used a dye-filled microcavity consisting of two spherical curved mirrors with radius of curvature R (see figure 1). These mirrors, placed opposite of each other, are separated by a distance D_0 along the optical axis. This means that at a distance r from the optical axis, the distance between the two mirrors is given by

$$D(r) = D_0 - 2\left(R - \sqrt{R^2 - r^2}\right). \tag{2}$$

Furthermore, the microcavity is filled with a drop of dye. This dye is very important because it thermalizes the photons via absorption and emission. Photons that leak out of the micro cavity are captured with a camera and this data can be used to analyze the BEC of photons. The total number of photons in the cavity is controlled by pumping with a laser with wavelength λ. Table 1 shows typical values for the experimental parameters.

R	$1m$
q	8
D_0	$2 \times 10^{-6}m$
λ	$523 \times 10^{-9}m$
m	$5.34 \times 10^{-36}kg$
Ω	$2.30 \times 10^{11}s^{-1}$
ω_{cut}	$3.18 \times 10^{15}s^{-1}$
l_{HO}	$9.27 \times 10^{-6}m$

Table 1: Typical values for the experiment.

2.2 Dispersion relation

To get a macroscopically occupied ground state, which is needed to obtain BEC, the curvature of the mirrors is very important. Free photons with frequency ω have of course a linear dispersion relation: $E = \hbar\omega$. However, in the cavity we can separate the momentum $\mathbf{k}$ of the photons into k_z along the optical axis of the mirrors and into k_r transversal to this optical axis. If furthermore $k_z \gg k_r$ we can approximate the energy of the photons:

$$E = \hbar c^*|\mathbf{k}| = \hbar c\sqrt{k_z^2 + k_r^2} \approx \hbar c^* \left(k_z + \frac{k_r^2}{2k_z}\right), \tag{3}$$

where c^* is the speed of light in the dye. The longitudinal momentum should satisfy the boundary condition $k_z(r) = q\pi/D(r)$ with q an integer that determines the wavenumber.
For $R \gg r$ and a fixed quantum number q we get the following approximated energy [2, 6]:

$$E \approx mc^{*2} + \frac{\hbar^2 k_r^2}{2m} + \frac{1}{2}m\Omega^2 r^2, \tag{4}$$

where we defined an effective photon mass

$$m = \frac{\hbar k_z(0)}{c^*} \tag{5}$$

and trapping frequency

$$\Omega = \frac{c^*}{\sqrt{D_0 R/2}}. \tag{6}$$

We can identify the first term with the rest energy [9]. The second term is proportional to the squared momentum, so we can identify it with the kinetic energy. For the last term, we recognize the harmonic potential (with trapping frequency Ω) for a massive particle in two spatial dimensions. So, instead of a linear dispersion relation as with free photons, we get a quadratic relation in r and a rest energy

$$E_0 = mc^{*2} = \hbar k_z(0)c^* = \hbar\omega_{cut}, \tag{7}$$

where we defined the cutoff frequency as

$$\omega_{cut} = k_z(0)c^*. \tag{8}$$

This means that the momentum k_z along the optical axis gives us a nonzero rest energy and we are left with a two-dimensional system (see figure 2).

2.3 Harmonic Oscillator

Equation (4) gives the energy of the photons in the cavity. We recognized that this equation is the same as for a massive particle (in this case a boson) in two spatial dimensions in a harmonic potential with trapping frequency Ω. This means that, in good approximation, the Hamiltonian H for photons in the BEC of light is given by (in Cartesian coordinates)

$$H = -\frac{\hbar^2}{2m}\nabla^2 + \frac{1}{2}m\Omega^2(x^2 + y^2). \tag{9}$$

Later on we will use this to choose variational wave functions. Therefore we need the normalized eigenstates ψ_{m_x,m_y} of the two-dimensional harmonic oscillator [10]:

$$\psi_{m_x,m_y}(x,y) = \frac{H_{m_x}\left(\frac{x}{l_{HO}}\right) H_{m_y}\left(\frac{y}{l_{HO}}\right) e^{-(x^2+y^2)/2l_{HO}^2}}{l_{HO}\sqrt{\pi 2^{m_x+m_y} m_x! m_y!}}, \tag{10}$$

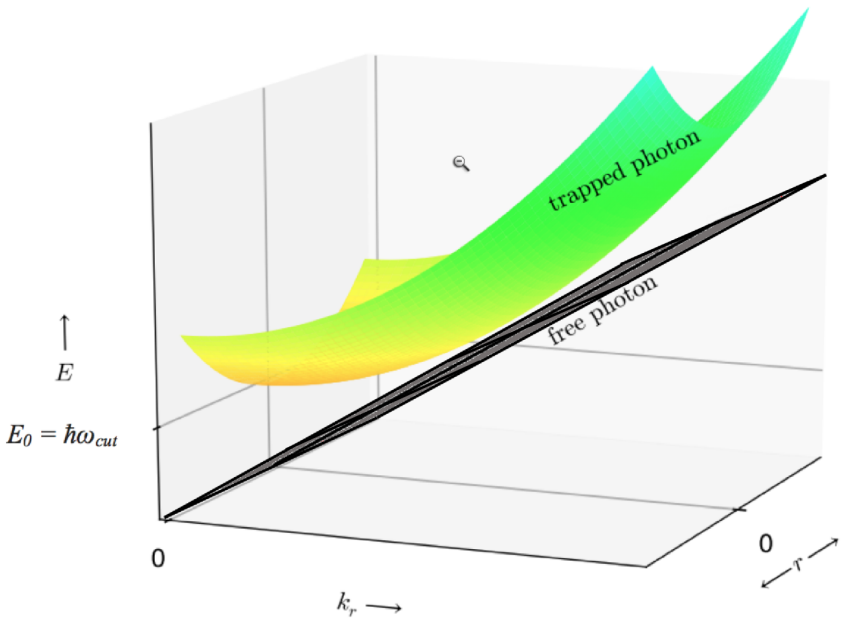

Figure 2: The energy dispersion relation of the trapped photon in the micro cavity as given by equation(4) [9]. To compare, the dispersion relation of a free photon is added in black. We see that on the optical axis of the micro cavity ($r = 0$) the energy of the trapped photon is lowest and given by equation (7)

.

where m_x, m_y are integers, $H_n(x)$ the n^{th} Hermite polynomial and the harmonic oscillator length is given by

$$l_{HO} = \sqrt{\frac{\hbar}{m\Omega}}. \tag{11}$$

From this, we immediately identify the typical length scale for a BEC of photons. (see table 1).

2.4 Effective interaction using the ground state

If we look at equation (10) we expect that the size of the condensate remains the same if the number of condensed photons changes and is equal to the harmonic oscillator length l_{HO}. However, it was measured that the condensate radius increases for larger condensate fractions [6]. The above Hamiltonian is the approximated equation to describe the BEC of light. A first simple improvement of this equation is to include a contact interaction for the particles (as essentially for long length scales every interaction is approximately a contact interaction). For BEC's the Gross-Pitaevskii equation is the common equation to include this interaction and to describe the ground state wave function $\psi(\mathbf{r})$ [6]. In van der Wurff et al. [8] and Greveling et al. [4] this contact interaction of the BEC of light was included via the following energy functional for the macroscopic wavefunction ϕ_0:

$$\Omega[\phi_0(\mathbf{r})] = \int d\mathbf{r}\phi_0(\mathbf{r})^* \left(\frac{\hbar^2}{2m}\nabla^2 + \frac{1}{2}m\Omega^2|\mathbf{r}|^2 - \mu + \frac{g}{2}|\phi_0(\mathbf{r})|^2 \right) \phi_0(\mathbf{r}), \tag{12}$$

where g is the coupling constant and μ the chemical potential. Here $\mathbf{r}$ denotes the two-dimensional position. They solved this equation with a variational ansatz similar to the ground state of the harmonic oscillator length:

$$\phi_0(\mathbf{r}) = \sqrt{N_0}\frac{1}{\sqrt{\pi}q}\exp\left(-|\mathbf{r}|^2/2q^2\right), \tag{13}$$

where the harmonic oscillator length l_{HO} has been replaced by the variational parameter q, which describes the width of the condensate.

c [mM]	$\tilde{g}$
1.50	$(12.4 \pm 1.3) \times 10^{-2}$
6.00	$(4.1 \pm 0.3) \times 10^{-2}$
10.5	$(1.5 \pm 0.1) \times 10^{-2}$
14.9	$(2.0 \pm 0.1) \times 10^{-2}$

Table 2: Dimensionless effective interaction $\tilde{g}$ for several dye concentrations [4].

Note that ϕ_0 has the following normalization condition for N_0 particles in the ground state:

$$\int d\mathbf{r}|\phi_0(\mathbf{r})|^2 = N_0. \tag{14}$$

Solving the energy functional variational, they found that the condensate radius was given by

$$R_c := q_{\min} = l_{HO}\sqrt[4]{1 + \frac{\tilde{g}N_0}{2\pi}}, \tag{15}$$

where they defined the dimensionless interaction strength

$$\tilde{g} = \frac{mg}{\hbar^2}. \tag{16}$$

Note that for small N_0 the condensate radius is close to the harmonic oscillator length l_{HO}. By fitting equation (15) with the data, $\tilde{g}$ can be determined (see figure 3). The results of Greveling et al. [4] for $\tilde{g}$ are listed in table 2 for several dye-concentrations. As discussed in section 1.2 we see that they found an effective interaction strength which is more then one order of magnitude larger than in previously experiments [6–8].

An explanation of this is that they measured the radius of the condensate and only assumed that the ground state was involved in the measurements. However, BEC's have always thermally occupied excited states and it is likely they contribute to the measured condensate size as well. When a too large condensate size is measured, it would therefore implicate that the effective interaction in table 2 is too large. This will be the motivation for the following section.

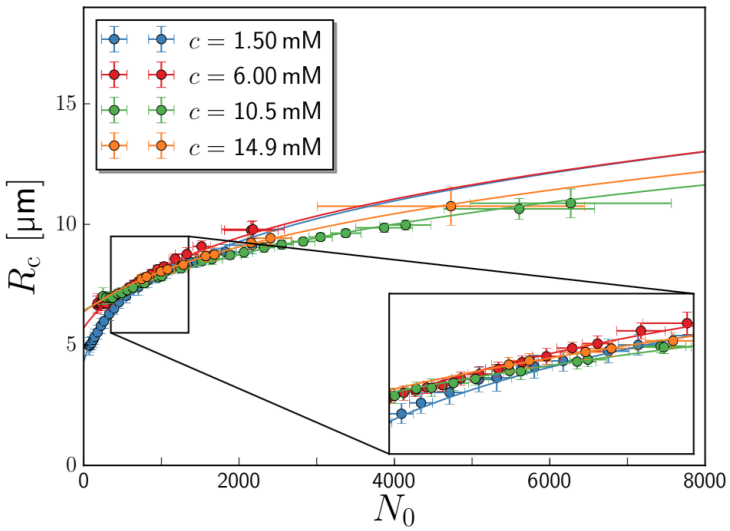

Figure 3: The condensate radius R_c as function of the number of condensate photons N_0. The dimensionless effective interaction $\tilde{g}$ is determined for several dye concentrations by fitting equation (15) to the data [4].

3 Condensate size as a measure for the interaction

As discussed in the previous section, the effective contact interactions of Greveling et al. [4] is likely an overestimation. In this section we will derive similar equations as equation (12) to describe the effective interaction for the ground state and an excited state. After that, we try to solve this with a variational ansatz for the ground and excited states. Our variational parameters are a direct measure for the condensate radius of the states. Because we can't find an analytical solutions we will use perturbation theory which can be done up to 11^{th} order. At the end of this section we will discuss our theoretical results. Moreover, we find limits to our model, which is the motivation for the next section.

3.1 Hartree-Fock approximation for two states

To derive equation (12) (which included a contact interaction for the ground state) one can use the Hartree-Fock approximation. To include the contact interaction for an excited state as well, we can use the Hartree-Fock approximation again to derive the following equations [11]:

$$\Omega_0 = \int d\mathbf{r}\psi_0^*(\mathbf{r}) \left[-\frac{\hbar^2}{2m}\nabla^2 + V(\mathbf{r}) - \mu + \frac{g}{2}|\psi_0(\mathbf{r})|^2 + 2g|\psi_1(\mathbf{r})|^2 \right] \psi_0(\mathbf{r}) \tag{17}$$

$$E_1 = \int d\mathbf{r}\psi_1^*(\mathbf{r}) \left[-\frac{\hbar^2}{2m}\nabla^2 + V(\mathbf{r}) + g|\psi_1(\mathbf{r})|^2 + 2g|\psi_0(\mathbf{r})|^2 \right] \psi_1(\mathbf{r}) \tag{18}$$

with μ the chemical potential. These equations are energy functionals for the ground state ψ_0 and the excited state ψ_1. The potential $V(\mathbf{r})$ is of course given by the harmonic trap:

$$V(\mathbf{r}) = \frac{1}{2}m\Omega^2|\mathbf{r}|^2 \tag{19}$$

where the effective mass m and the trap frequency Ω are discussed in section 2.2. The difference of $\frac{g}{2}|\psi_0(\mathbf{r})|^2$ and $g|\psi_1(\mathbf{r})|^2$ comes from the symmetric two-particle wave function, needed for bosons. Note furthermore the exchange terms $2g|\psi_1(\mathbf{r})|^2$ and $2g|\psi_0(\mathbf{r})|^2$ for equations (17) and (18) respectively.

3.2 Variational approach

We solve these equations variational [10]. To do this we have to choose our wave functions carefully. In sections 2.2 and 2.3 we discussed that in good approximation the external potential for a BEC of light looks like that of the harmonic oscillator. In the above equations we only added a contact interaction, which is presumable small [6]. A good choice for our variational wave functions would therefore be functions that are a small deviation of the eigenstates of the harmonic oscillator. From the experiment, we know that modes like the $n_x = n_y = 0$ and the $n_x = n_y = 1$ can be measured separately. We discussed earlier that the condensate size increases when more particles are in the BEC. So, it is a good approach to choose variational parameters which are a measure for the size. Therefore we start with the following variational ansatz:

$$\psi_0(x,y) = \sqrt{N_0} \cdot \frac{1}{\sqrt{\pi}q_0} \exp\{-(x^2+y^2)/q_0^2\} \tag{20}$$

$$\psi_1(x,y) = \sqrt{N_1} \cdot \frac{2}{\sqrt{\pi}q_1^3} xy \exp\{-(x^2+y^2)/q_1^2\} \tag{21}$$

Of course, we don't expect that the two wave functions have the same size. That's why we defined the variational parameters q_0 and q_1. These parameters are a direct measure of the size of these wave functions. Note that ψ_0 is the same wave function for the ground state as in section 2.4. The wave functions are normalized to the number of photons N_0 in the ground state and the number of photons N_1 in the excited state respectively.

Now solving the integrals of equations (17) and (18) for these wave functions gives:

$$\tilde{\Omega}_0 = \frac{N_0}{2\tilde{q}_0^2} + \frac{1}{2}N_0\tilde{q}_0^2 - \tilde{\mu}N_0 + \frac{\tilde{g}N_0^2}{4\pi\tilde{q}_0^2} + \frac{2\tilde{g}N_0N_1\tilde{q}_0^4}{\pi(\tilde{q}_0^2+\tilde{q}_1^2)^3}, \tag{22}$$

$$\tilde{E}_1 = \frac{3N_1}{2\tilde{q}_1^2} + \frac{3}{2}N_1\tilde{q}_1^2 + \frac{9\tilde{g}N_1^2}{32\pi\tilde{q}_1^2} + \frac{2\tilde{g}N_0N_1\tilde{q}_0^4}{\pi(\tilde{q}_0^2+\tilde{q}_1^2)^3}, \tag{23}$$

where we defined the dimensionless parameters

$$\tilde{q}_0 = \frac{q_0}{l_{HO}}, \qquad \tilde{q}_1 = \frac{q_1}{l_{HO}}, \qquad \tilde{g} = \frac{mg}{\hbar^2},$$
$$\tilde{\mu} = \frac{\mu}{\hbar\omega}, \qquad \tilde{\Omega}_0 = \frac{\Omega}{\hbar\omega}, \qquad \tilde{E}_1 = \frac{E_1}{\hbar\omega}.$$

Experimentally, one has only control over the pump laser to change the total number of photons $N = N_0+N_1$. However, it isn't possible to tune N_0 and N_1 separately. The total number N isn't easy to determine because only a fraction of the particles leak out of the cavity and are captured on the camera. Therefore we could add an unknown scaling parameter, or rewrite our equations in terms of the well-defined polarization

$$p = \frac{N_1 - N_0}{N_0 + N_1}. \tag{24}$$

Rewriting equations (22) and (23) in terms of p and N gives:

$$\tilde{\Omega}_0 = \frac{N}{2}\left[\frac{1-p}{2\tilde{q}_0^2} + \frac{1}{2}(1-p)\tilde{q}_0^2 - \tilde{\mu}(1-p) + \frac{\tilde{g}N(1-p)^2}{8\pi\tilde{q}_0^2} + \frac{\tilde{g}N(1-p^2)\tilde{q}_0^4}{\pi(\tilde{q}_0^2+\tilde{q}_1^2)^3}\right], \tag{25}$$

$$\tilde{E}_1 = \frac{N}{2}\left[\frac{3(1+p)}{2\tilde{q}_1^2} + \frac{3}{2}(1+p)\tilde{q}_1^2 + \frac{9\tilde{g}N(1+p)^2}{64\pi\tilde{q}_1^2} + \frac{\tilde{g}N(1-p^2)\tilde{q}_0^4}{\pi(\tilde{q}_0^2+\tilde{q}_1^2)^3}\right]. \tag{26}$$

By using the variational principle we should minimize these equations with respect to $\tilde{q}_0$ and $\tilde{q}_1$. However, it is not possible to find an analytical solution for $\tilde{q}_0$ and $\tilde{q}_1$. Nevertheless, note that the unknown $\tilde{g}$ and the not so easy to measure N are now packed into one unknown $\tilde{g}N$. In the next subsection we will use this fact to find a solution for $\tilde{q}_0$ and $\tilde{q}_1$.

3.3 Solution

Because the above equations have no analytical solutions we use perturbation theory to find a solution [10]. Therefore we write $\tilde{q}_0$ and $\tilde{q}_1$ as a power series in the unknown $\tilde{g}N$, with coefficients $q_0^{(i)}$ and $q_1^{(i)}$ for $0 \le i < \infty$:

$$\tilde{q}_0 = \sum_{i=0}^{\infty} q_0^{(i)}(\tilde{g}N)^i, \tag{27}$$

$$\tilde{q}_1 = \sum_{i=0}^{\infty} q_1^{(i)}(\tilde{g}N)^i. \tag{28}$$

Up to second order this gives

$$\tilde{q}_0 = 1 + \frac{1-3p}{32\pi}\tilde{g}N - \frac{3(1-6p+9p^2)}{2048\pi^2}(\tilde{g}N)^2 + \mathcal{O}((\tilde{g}N)^3), \tag{29}$$

$$\tilde{q}_1 = 1 + \frac{7-p}{128\pi}\tilde{g}N - \frac{3(49-14p+p^2)}{32768\pi^2}(\tilde{g}N)^2 + \mathcal{O}((\tilde{g}N)^3). \tag{30}$$

Note that for the linear term we have $q_{0,1}^{(1)} \simeq 10^{-2}$ and for the second term $q_{0,1}^{(1)} \simeq 10^{-3}$. So, even for $\tilde{g}N$ of the order of 1, the lengths are just small modifications of the harmonic oscillator length. It is possible

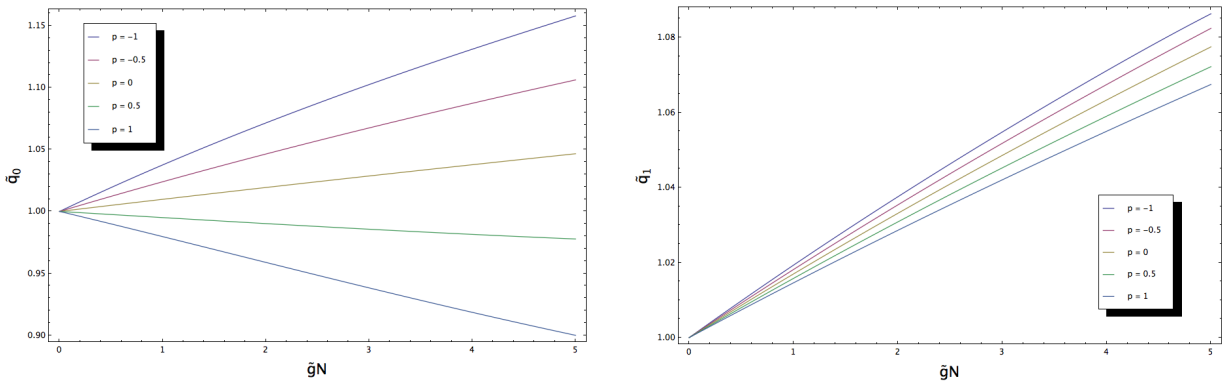

(a) (b)

Figure 4: Condensate radius $\tilde{q_0}$ and $\tilde{q_1}$ (scaled in units of the harmonic oscillator length l_{HO}) of the ground state and excited state respectively as function of $\tilde{g}N$ for several values of the polarization p. **(a)** For low values of p, the radius increases for larger total numbers. However, for $p \geq \frac{1}{3}$ the condensate radius decreases for increasing total numbers. **(b)** The radius of the excited state gets smaller for increasing polarization.

to go up to 11^{th} order, but these higher orders are even smaller then the ones just given. However, for fine convergence of the results, we will use the answers for 11^{th} order from now on.

Let's take a better look at our solutions. In figure 4a we see $\tilde{q_0}$ for various values of the polarization p. First we notice the almost linear behavior of $\tilde{q_0}$, which we expected. For low values of the polarization we see that, as mentioned before in the different studies [4, 6], the condensate radius increases for larger condensate numbers. However, for more particles in the excited state, the condensate radius $\tilde{q_0}$ of the ground state decreases. If $p \geq \frac{1}{3}$ we see that $\tilde{q_0}$ becomes smaller then 1. This means that when many particles are in the excited state with respect to the number of particles in the ground state, we get a ground state size which is even smaller then the harmonic oscillator length l_{HO}. This is a consequence of the repulsive interaction. We will discuss this effect in the next subsection. Furthermore, we notice that for this polarization the condensate radius decreases for increasing condensate numbers.

If we look at figure 4b we see also that for more particles in the excited state, the condensation radius $\tilde{q_1}$ of the excited state gets smaller. This is a result of the repulsive interaction as well. However, as happened with $\tilde{q_0}$, there is no polarization for which $\tilde{q_1}$ decreases for larger total numbers.

3.4 Discussion

We have seen now what our solutions of the condensate radius $\tilde{q_0}$ and $\tilde{q_1}$ for the different values of polarization look like. To understand what happens for the different values of polarization and what it has to do with the repulsive interaction of the photons, we need to take a look at the spatial form of our variational ansatz. In figure 5 we have plotted $|\psi_0|^2$ (in yellow) and $|\psi_1|^2$ (in red) for different values of the polarization. We can divide our discussion into two situations. On the one hand, polarizations $p \leq \frac{1}{3}$ where the ground state increases for larger $\tilde{g}N$. On the other hand, polarizations $p \geq \frac{1}{3}$ where the ground state size decreases.

3.4.1 Small polarization ($p \leq \frac{1}{3}$)

First notice that for small values of polarization, the ground state is relatively more peaked then the excited state (figures 5a and 5b). The repulsive interaction of the photons has as a consequence that the wave function of the ground state (which is a Gaussian centered at the origin), presses the excited state outside. So this repulsive interaction between the photons not only results in a larger radius q_0 for the ground state (at least for $p \leq \frac{1}{3}$), but it results also in a larger radius q_1 of the excited state (see also figure 4), because this state is pressed away from the ground state.

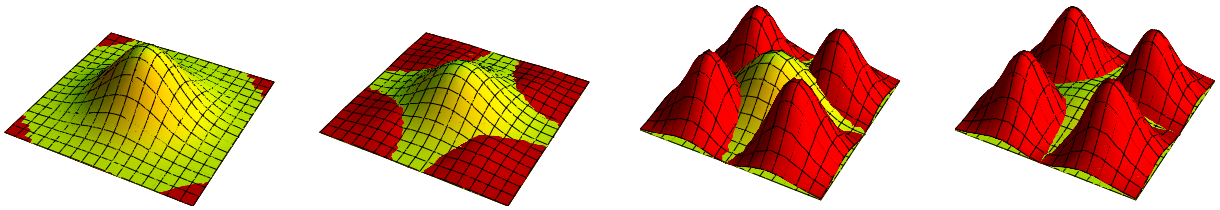

(a) (b) (c) (d)

Figure 5: Relative plots of $|\psi_0|^2$ (in yellow) and $|\psi_1|^2$ (in red) for different values of polarization (see also equations (20) and (21)): **(a)** $p = -0.5$, **(b)** $p = 0.2$, **(c)** $p = 0.5$ and **(d)** $p = 0.7$.

3.4.2 Large polarization ($p \geq \frac{1}{3}$)

For larger polarization though, the excited state has a spatial form which is relatively more peaked then the ground state (figures 5c and 5d). The quadrupole form of the excited state, presses the photons in the ground state closer together. When enough photons are in the excited state (this happens when $p \geq \frac{1}{3}$), equations (29) and (30) even predict a decreasing radius q_0, smaller then the harmonic oscillator length l_{HO} for the ground state. The reason we didn't find a decreasing q_1 as we did for q_0, is because the quadrupole form of the excited state lies outside the Gaussian form of the ground state. So, when more particles are add in the excited state, it still has room to expand.

3.4.3 Comparison with one mode

We can compare our results with the condensate radius R_c found in section 2.4 used by Greveling et al. [4]. First of all, we should obtain the same results for the polarization $p = -1$. Then $N_1 = 0$ and the effect of the excited state vanishes, so it shouldn't alter the condensate radius. In figure 6a, $\tilde{q_0}$ is plotted up to 2^{nd} and 11^{th} together with the analytical result R_c. From the figure, we determine that our solution for $\tilde{q_0}$ converges to the analytical result R_c when more terms are added. It is good to say that the convergence is slowest for the extreme polarization $p = -1$.

If we look at figure 5, we see that the excited state lies around the ground state. Because in Greveling et al. [4] this state was also included in the ground state they clearly found a too large condensation radius. As we discussed earlier, this implicates indeed a too large effective interaction.

However, what is the difference between the model for R_c and our model for two states when one is able to measure the radius q_0 of the ground state without the disturbance of the excited state? Because we expect a polarization higher then $p = -1$, our model predicts that the condensate radius of the ground state won't expand as fast as was predicted by equation (15) for R_c (see also figure 4). This means that when one measures only q_0 and fits this to the equation of R_c he finds another effective interaction $\tilde{g}$ then when he fits it to our model for two states. The difference of these two models is shown in figure 6b. In this figure we plotted for fixed N_0 the difference of the effective interaction $\Delta\tilde{g} = \tilde{g}_{\text{one}} - \tilde{g}_{\text{two}}$ as function of p. Here $\tilde{g}_{\text{one}}$ is the effective interaction when q_0 is fitted to R_c and $\tilde{g}_{\text{two}}$ the effective interaction which follows from fitting q_0 to our model for two states. We did this for several values of $\tilde{q_0}$. Not that this works until p exceeds the critical value $\frac{1}{3}$ because then our model for two states predicts that q_0 is even smaller then the harmonic oscillator length l_{HO}. We conclude that when one can measure the radius of the ground state separately, our model for two states predicts a larger effective interaction then the model R_c for one state.

3.4.4 Limits of the model

For now, when we know p, $q_{0,1}$ and N our model (equations (29) and (30)) gives us a way to determine the effective interaction $\tilde{g}$ (see also section 5). These are all parameters which can be experimental determined. As we saw above, q_0 and q_1 are strongly dependent on the polarization. Therefore, it would be nice if we could say something about this. However, without knowing the effective interaction, our model isn't sufficient to say something about the polarization yet. This leaves us with our second research question: *what describes the photon occupation numbers of different states in the BEC of light and how does it depend on the pump*

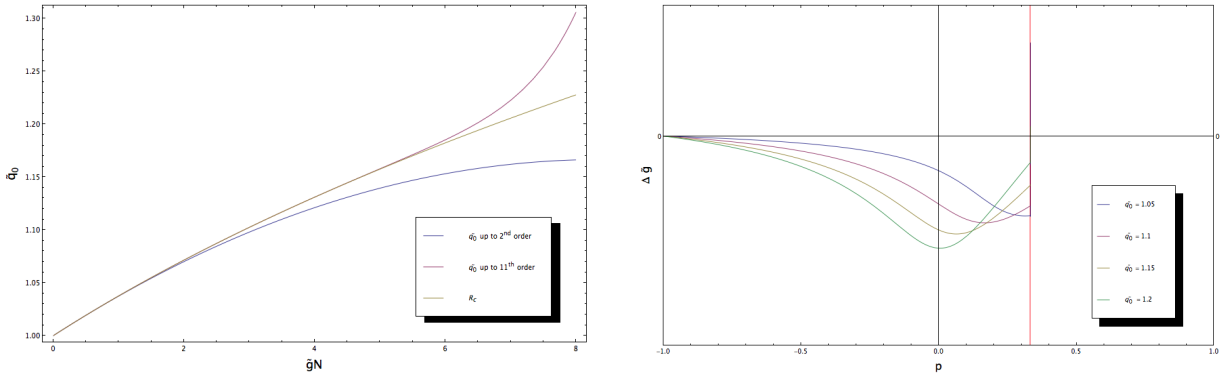

(a) (b)

Figure 6: **(a)** Plot of $\tilde{q_0}$ for $p = -1$ up to 2^{nd} and 11^{th} order together with the analytical result R_c. **(b)** The effective interaction $\Delta\tilde{g} = \tilde{g}_{\text{one}} - \tilde{g}_{\text{two}}$ as function of p for fixed N_0. Here $\tilde{g}_{\text{one}}$ is the effective interaction when q_0 is fitted to R_c and $\tilde{g}_{\text{two}}$ the effective interaction fitted to our model for two states.

laser? First of all, we expect that the profile and the rate of the pump laser must be taken into account before we can understand the polarization. This is because the pump sets the total number N of photons in the system. Besides, the pump rate could cause one state to increase relative to the other. To include this, we need to have a better understanding of the pump laser and how it effects the distribution of the different states.

3.5 Conclusion

We have found a way, when N_0 and N_1 are known, to obtain the dimensionless effective interaction $\tilde{g}$ from the radii q_0 and q_1 of the ground state and the excited state, respectively. The quadrupole form of the excited state decreases the radius of the ground state. We identified the critical value $p \geq \frac{1}{3}$, where this effect is so large that the radius of the ground state even gets smaller then the harmonic oscillator length l_{HO}. On the other hand, the radius of the excited state is always increased by the Gaussian form of the ground state which presses the excited state away from the origin. Of course, inclusion of another excited state may change this conclusion. When one is able to measure q_0 without the disturbance of the excited state, our model predicts a larger effective interaction than the model R_c for one state. However, we still expect a smaller effective interaction then Greveling et al. [4] because as discussed, they measured a condensate radius which was too large. Finally, we identified that our model isn't able to describe the photon numbers of the different states. We will look at this in the next section.

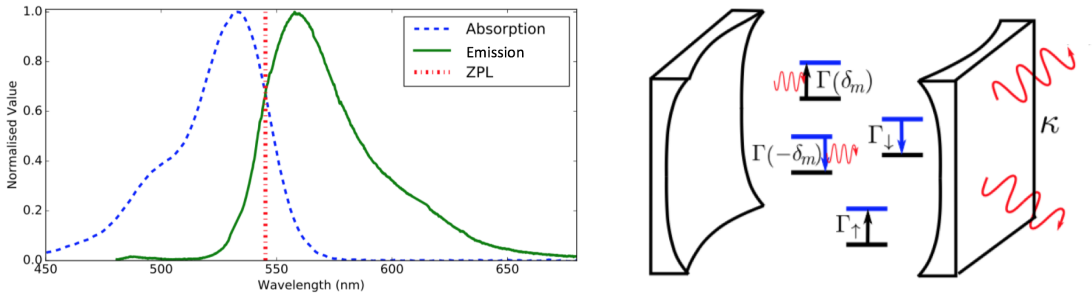

(a) (b)

Figure 7: **(a)** The absorption and emission spectra for the dye. Both are normalized to their peak value and the ZPL is the wavelength at which they are equal [5]. **(b)** schematic picture of the different rates for the photons [12]

4 Photon numbers

As discussed at the end of the previous section, we are not able to predict the polarization yet. In this section we will look how the pump laser effects the polarization. Before we do this, we explore the physically important phenomena of the photon condensate. From this, one can derive equations which describe the photon number and the excitation density of the dye molecules. We discuss these equation to understand how the phenomena of the condensate are linked together. After that, we make certain approximations to find solutions of our equations. At the end of this section, we will discuss these results and look at the dependence of the photon occupation numbers on the pump laser.

4.1 Physical understanding of the condensate

In the condensate, equilibrium is reached as the photons are absorbed and emitted by the dye molecules [2]. Of course, we can predict the polarization by complete knowledge of how the photons interact with the dye. However, the dye molecules have complex optical spectra and therefore complete knowledge of the dye is unfeasible. In this subsection we will identify the basic physics to understand the phenomena that are important for the photon condensate. In figure 7b a schematic picture of these phenomena is given.

4.1.1 Absorption and emission rates of the dye

Despite this incomplete knowledge of the dye, one can treat the molecules as a two-level system with two electronic states, the highest occupied molecular orbital (HOMO) and the lowest unoccupied molecular orbital (LUMO). Because these levels are dressed by ladders we can identify absorption and emission rates $\Gamma(\delta_m)$ and $\Gamma(-\delta_m)$ respectively [12]. Here δ_m is the detuning, of state m in the photon system, from the Zero Phonon Line (ZPL) of the dye molecule:

$$\delta_m = \epsilon_m - \epsilon_{ZPL} \tag{31}$$

As discussed, the photon states are in good approximation given by the eigenstates of the Harmonic oscillator (equation (10)). This means that $m = m_x + m_y$ and as discussed in section 2.2 we can write

$$\epsilon_m = E_0 + (m_x + m_y + 1)\hbar\Omega, \tag{32}$$

where $E_0 = \hbar\omega_{cut}$ is the rest energy. Typical spectra of absorption and emission for the dye are shown in figure 7a. The absorption and emission rates follow the Kennard-Stepanov relation [5, 12]. This relation is dictated by a principle of detailed balance, namely

$$\frac{\Gamma(\delta_m)}{\Gamma(-\delta_m)} = e^{\beta\delta_m}. \tag{33}$$

4.1.2 Cavity and non-cavity decay rates of the dye

Photons can leave the system in two ways. First of all, photons leak out of the cavity. These photons are captured on the camera and can be used to analyze the condensate. We assume that every mode m has the same cavity decay rate κ. On the other hand, dye molecules can have a non-cavity decay rate, because they decay into other states than the confined cavity modes. Because they aren't interesting to us anymore we don't have to specify these states. It is therefore enough to denote this by the non-cavity decay rate $\Gamma_\downarrow$.

4.1.3 Pumping rate

To make up for the non-cavity decay rate $\Gamma_\downarrow$ of the dye molecules, they are excited with a pump laser. We denote the pumping rate by $\Gamma_\uparrow(\mathbf{r})$. The coordinate dependence $\mathbf{r}$ is included because not only its rate is important, but also the profile of the pump. In this section we will use a Gaussian pump spot, centered at the origin:

$$\Gamma_\uparrow(\mathbf{r}) = \Gamma_\uparrow e^{-\mathbf{r}^2/2\sigma^2}, \tag{34}$$

where $\Gamma_\uparrow$ is the actual rate and σ is the spot size. Of course, in the following equations other pump spots can be used.

4.2 Photon numbers and excitation density

Now that we understand the processes that take place in the photon system, we can link them together and try to understand the polarization. In the theoretical work of Keeling and Kirton [12], the above parameters are connected into coupled equations that describe the number n_m of photons in state m and the excitation density $f(\mathbf{r})$ of the dye molecules:

$$\frac{\partial n_m}{\partial t} = \rho_0 \Gamma(-\delta_m) f_m (n_m + 1) - \left[\kappa + \rho_0 \Gamma(\delta_m)(1 - f_m)\right] n_m \tag{35}$$

$$\frac{\partial f(\mathbf{r})}{\partial t} = -\Gamma_\downarrow^{\mathbf{tot}}(\{n_m\}, \mathbf{r}) f(\mathbf{r}) + \Gamma_\uparrow^{\mathbf{tot}}(\{n_m\}, \mathbf{r})(1 - f(\mathbf{r})) \tag{36}$$

where ρ_0 is the density of dye molecules. The equations are coupled via the fractions f_m for the different states m defined by

$$f_m = \int d\mathbf{r} f(\mathbf{r}) |\psi_m(\mathbf{r})|^2, \tag{37}$$

and the total rates

$$\Gamma_\downarrow^{\mathbf{tot}}(\{n_m\}, \mathbf{r}) = \Gamma_\downarrow + \sum_m |\psi_m(\mathbf{r})|^2 \Gamma(-\delta_m)(n_m + 1), \tag{38}$$

$$\Gamma_\uparrow^{\mathbf{tot}}(\{n_m\}, \mathbf{r}) = \Gamma_\uparrow(\mathbf{r}) + \sum_m |\psi_m(\mathbf{r})|^2 \Gamma(\delta_m) n_m. \tag{39}$$

Although we gave the equations without derivation, we can still have a look and try to understand the physics behind them. First of all, equation (35) describes the occupation of the different photon states. As we discussed above, the photons interact with the dye via absorption and emission and these processes alter the photon occupation numbers n_m. Only the fraction f_m of excited dye molecules can emit a photon and when a dye molecule emits a photon of state m, the number n_m is increased by 1. This results in the term $f_m(n_m + 1)$. Multiplying this with the rate of emission $\Gamma(-\delta_m)$ and the dye density ρ_0, yields the change in time for the emission. However, absorption of one of the n_m photons in state m can only happen for the fraction $1 - f_m$ of dye molecules. Therefore, we get for absorption rate $\Gamma(\delta_m)$, the term $-\rho_0\Gamma(\delta_m)(1 - f_m)n_m$ (we get a minus sign because the photon is absorbed by a dye molecule). Because all photons have the same cavity decay rate κ, the term $-\kappa n_m$ speaks for itself.

Equation (36) describes the excitation density. The density $f(\mathbf{r})$ of excited dye molecules is decreased by $\Gamma_{\downarrow}^{\mathbf{tot}}(\{n_m\},\mathbf{r})$ which is given in equation (38). As expected, two things can happen. On the one hand, emission into cavity modes which is indicates by the sum over the states m. This emission has for state m rate $\Gamma(-\delta_m)$ and just as above, the number n_m of state m is increased by one. On the other hand, decay into other states than the confined cavity states can happen, which we denoted earlier by the rate $\Gamma_{\downarrow}$. The excitation density increases by exciting the fraction $1-f(\mathbf{r})$. This happens with rate $\Gamma_{\uparrow}^{\mathbf{tot}}(\{n_m\},\mathbf{r})$ given in equation (39). It is the sum of the absorption rates $\Gamma(\delta_m)$ and the pump rate $\Gamma_{\uparrow}(\mathbf{r})$. The non-excited dye molecules can be excited by absorbing one of the n_m photons from the condensate. The total absorption density is of course given by multiplying with $|\psi_m|^2$ and taking the sum over m.

4.3 Equilibrium

The equations above can't be solved analytical. However, we are interested in the equilibrium situation and in that case the equations simplify. In the equilibrium situation, one can set:

$$\frac{\partial n_m}{\partial t}=0 \qquad \text{and} \qquad \frac{\partial f(\mathbf{r})}{\partial t}=0. \tag{40}$$

From this, we can solve equations (35) and (36) for n_m and $f(\mathbf{r})$, leading to

$$n_m=\frac{\rho_0\Gamma(-\delta_m)f_m}{\kappa-\rho_0\Gamma(-\delta_m)f_m+\rho_0\Gamma(\delta_m)(1-f_m)}, \tag{41}$$

$$f(\mathbf{r})=\frac{\Gamma_{\uparrow}^{\mathrm{tot}}(\{n_m\},\mathbf{r})}{\Gamma_{\uparrow}^{\mathrm{tot}}(\{n_m\},\mathbf{r})+\Gamma_{\downarrow}^{\mathrm{tot}}(\{n_m\},\mathbf{r})}. \tag{42}$$

The rates $\Gamma(\pm\delta_m)$ should follow the principle of detailed balance given in equation (33). This gives for the photon occupation numbers

$$n_m=\frac{1}{\frac{\kappa}{\rho_0\Gamma(-\delta_m)f_m}+\frac{1-f_m}{f_m}e^{\beta\delta_m}-1}. \tag{43}$$

Note that we obtained a equilibrium distribution which looks similar to the Bose-Einstein distribution.

4.4 Large pump spot and background decay

The above equations for $f(\mathbf{r})$ and n_m don't have analytical solutions for the harmonic-oscillator eigenstates. However, it is still interesting to look at some limits. First of all, we look at the case that the background decay rate $\Gamma_{\downarrow}$ is much larger then the emission rates $\Gamma(-\delta_m)$ for the different modes. In this case we get

$$\Gamma_{\downarrow}^{\mathbf{tot}}(\{n_m\},\mathbf{r})\approx\Gamma_{\downarrow}. \tag{44}$$

Secondly, we look at the limit of a large pump rate. So the excitation of the dye molecules happens mainly by the pump spot. This gives:

$$\Gamma_{\uparrow}^{\mathbf{tot}}(\{n_m\},\mathbf{r})\approx\Gamma_{\uparrow}(\mathbf{r}) \tag{45}$$

The last approximation we want to add is that of a large pump spot size $\sigma\gg l_{HO}$. Then, the Gaussian pump looks almost constant with respect to the wave functions ψ_m. With this we can simply compute f_m as

$$f_m=\int d\mathbf{r}f(\mathbf{r})|\psi_m\mathbf{r}|^2\approx\int d\mathbf{r}\frac{\Gamma_{\uparrow}}{\Gamma_{\uparrow}+\Gamma_{\downarrow}}|\psi_m(\mathbf{r})|^2=\frac{\Gamma_{\uparrow}}{\Gamma_{\uparrow}+\Gamma_{\downarrow}}, \tag{46}$$

where we used the normalization condition of $\psi_m(\mathbf{r})$. Note that the excitation fractions f_m are independent of m. Physically, this means that the pump laser excites the dye molecules evenly for the different states.

We obtain now

$$n_m = \frac{1}{\eta_m \frac{(\Gamma_\uparrow + \Gamma_\downarrow)}{\Gamma_\uparrow} + \frac{\Gamma_\downarrow}{\Gamma_\uparrow} e^{\beta \delta_m} - 1}, \tag{47}$$

where we defined the quantity

$$\eta_m = \frac{\kappa}{\rho_0 \Gamma(-\delta_m)}. \tag{48}$$

We see that with above limits the numbers n_m only differ by the emission rate $\Gamma(-\delta_m)$ and the detuning δ_m with respect to the ZPL.

4.5 Discussion

Now we have found some results for the photon occupation numbers n_m it's time to interpret them. We are interested in the dependence on the pump rate, because this is experimentally the parameter to control the number of photons in the condensate. To fully understand the dependence on the pump and which other parameters are important it's good to look at some limits.

4.5.1 No cavity decay

Let's first have a look at the ideal situation of zero cavity decay. This happens when $\kappa \to 0$ and we get a distribution of n_m that looks very similar to a Bose-Einstein distribution

$$n_m = \frac{1}{\frac{\Gamma_\downarrow}{\Gamma_\uparrow} e^{\beta \delta_m} - 1}, \tag{49}$$

where the condition for a Bose-Einstein distribution is the following:

$$\frac{\Gamma_\downarrow}{\Gamma_\uparrow} e^{\beta \delta_m} = e^{\beta(\epsilon_m - \mu)}, \tag{50}$$

with μ the chemical potential of the dye molecules. Solving this for μ gives, using $\delta_m = \epsilon_m - \eta_{ZPL}$

$$\mu = \epsilon_{ZPL} + k_b T \log\left(\frac{\Gamma_\uparrow}{\Gamma_\downarrow}\right). \tag{51}$$

When μ reaches the lowest photon energy $E_0 + \hbar\Omega$ from below, a Bose-Einstein condensate is realized [5]. This happens for the pump rate

$$\Gamma_\uparrow = \Gamma_\downarrow e^{\beta \delta_{cut}}, \tag{52}$$

with δ_{cut} the detuning of the lowest energy $E_0 + \hbar\Omega$ with respect to the ZPL. This rate is also known as the threshold pump rate because at this pump rate Bose-Einstein condensation sets in and we get a macroscopically occupied ground state.

4.5.2 Small pump rate

In the limit of small pump rate $\frac{\Gamma_\downarrow}{\Gamma_\uparrow} \gg 1$, the photon number is approximately given by

$$n_m \approx \frac{\Gamma_\uparrow}{\Gamma_\downarrow} \frac{1}{\eta_m + e^{\beta \delta_m}}. \tag{53}$$

When also $\eta_m \ll e^{\beta \delta_m}$, so the cavity decay κ is relatively small with respect to the emission rates, we get

$$n_m \approx \frac{\Gamma_\uparrow}{\Gamma_\downarrow} e^{-\beta \delta_m}. \tag{54}$$

From the Boltzmann factor that arises, we conclude that we are left with a classical thermal photon distribution. However, when the cavity decay is relatively large, $\eta_m \gg e^{\beta \delta_m}$, the thermalization fails. The reason

for this is that κ is larger then the emission rate. So the emitted photons are likely to immediately leave the cavity and there is no time for the photons to thermalize. In this regime we obtain

$$n_m \approx \frac{\Gamma_\uparrow}{\eta_m \Gamma_\downarrow}. \tag{55}$$

This shows the great dependence of the n_m on η_m. We will explore this dependence further in a moment. Note that in both cases the number of photons grow linear with the pump rate $\Gamma_\uparrow$.

4.5.3 Threshold pump rate

Above we found the threshold pump rate at which Bose-Einstein condensation is realized for the ideal situation with no cavity decay κ. However, when κ can't be ignored, we expect that the laser must pump harder to compensate for the cavity loss. When the denominator of equation (43) (almost) vanishes, we get of course macroscopically occupied states. This happens for the threshold pump power

$$\Gamma_\uparrow^{\text{tresh}} = \Gamma_\downarrow \frac{e^{\beta\delta_m} + \eta_m}{1 - \eta_m}. \tag{56}$$

Let's have a look at the dependence of η_m. For $\eta_m = 0$ we get the same result of equation (52). In figure 8 we plotted n_m as a function of the pump rate $\Gamma_\uparrow$. The blue and red lines are values of $\eta_m < 1$. We see that as the pump rate increases the photon number diverges. This phenomena is called lasing. When η_m is just below one, equation (56) predicts that lasing only sets in for very large pump rates. This is expected because in that case the cavity decay is so large that almost every emitted photon by the dye molecules leaves immediately the cavity. Furthermore, it shouldn't come as a surprise that this threshold pump rate will be greater when the background decay $\Gamma_\downarrow$ is large. The vertical lines show the threshold pump rate for which the denominator of equation (43) has vanished.

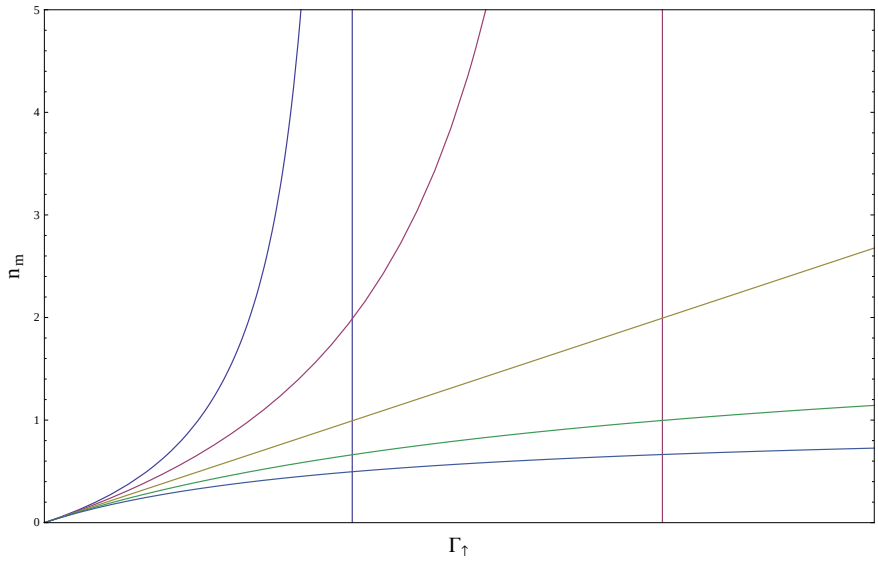

Figure 8: We see the photon occupation numbers n_m as function of the pump rate $\Gamma_\uparrow$ for several values of η_m. For $\eta_m \leq 1$ lasing is observed, which is shown by the blue and red lines. The yellow line is the case in which $\eta_m = 1$. Then, the photon number is linear with the pump rate. For larger η_m, the photon number converges to a fixed value.

For the critical value $\eta_m = 1$ the denominator can't vanish and the photon number is linear in the pump rate and given by

$$n_m = \frac{\Gamma_\uparrow}{\Gamma_\downarrow(1 + e^{\beta\delta_m})}. \tag{57}$$

This is shown by the yellow line. When $\eta_m \geq 1$, we get photon occupation numbers that converge to a finite value. This is shown by the green and the light blue lines. This asymptote is equal to

$$n_m \to \frac{1}{\eta_m - 1}. \tag{58}$$

So for η_m slightly above 1, we still can get macroscopically occupied states. Note furthermore, that once the threshold pump rate is exceeded for a state with $\eta_m < 1$, the denominater of equation (43) gets negative and so the photon number for this state makes no sense anymore. We expect that in these cases our approximations aren't valid anymore and it's likely that the emission/absorption rates and the spatial form of the states (see equations (38) and (39)) must be taken into account. This has been confirmed in Keeling and Kirton [12] where they also looked just above threshold. They observed for these limits phenomena as gain clamping of the excitation density and spatial hole burning.

4.6 Conclusion

In this section we discussed the physically phenomena in the cavity which led to the definition of several rates. We linked these rates together via coupled rate equations. These equations describe the photon occupation numbers of the states and the excitation density of the dye molecules. Although these equations don't have an analytic solution, they gave us much insight in the important things to describe the photon distribution.

Nevertheless, we tried to solve the equation in equilibrium with certain approximations. These approximations from section 4.4 gave some insight in what should happen when the background decay and pump rate is much larger then the emission and absorption rates. In this case we found that for small pump rates the photon occupation numbers depend linear on the pump rate. If this linear behavior is thermal depends on the energy of the photon state. We also derived the chemical potential at which Bose-Einstein condensation sets in for the ideal case of no cavity decay. Inspired by this, we tried to find critical pump rates for which this also happens when cavity decay is important. We found a result which was strongly dependent on the ratio of emission of the dye molecules and cavity decay. When the cavity decay is relatively small, we expect lasing for the photon state. However, when the cavity decay is relatively larger, the emitted photons will leave the cavity before they can thermalize and the photon number reaches a finite value. From this we can conclude that not only the dependence on the pump rate is important for the photon occupation numbers, but also the cavity decay and the emission and absorption rates of the dye. When in the experiment the cavity decay can be tuned we expect that both lasing and finite photon occupation numbers can be observed.

In the case of lasing, when the threshold pump rates is exceeded, our model isn't valid anymore. This is likely due to the fact we didn't fully include the emission/absorption rates and ignored the spatial form of the cavity modes.

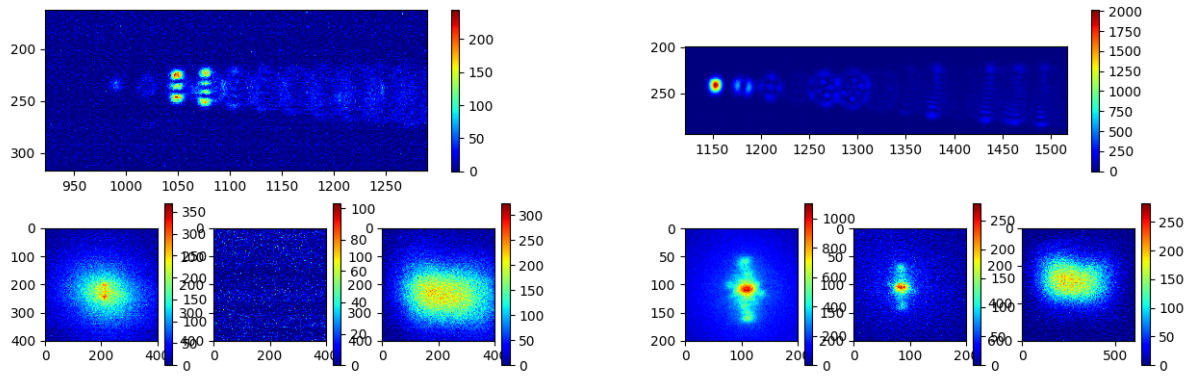

(a) (b)

Figure 9: Typical measurements on the Bose-Einstein condensate. Photons that leak out of the cavity are captured with a camera. The color and intensity of the pictures are parameters for the different modes and number of photons in the system respectively. The condensate radius can be measured from these pictures in units of pixels. On the left we see a measurement for the ground state and on the right, the excited state is measured.

5 Comparison with experiment

In this section, we compare our theoretical results from the previous two sections with experimental data. In section 3 we found equations for the condensate radius $\tilde{q_0}$ and $\tilde{q_1}$ of our variational ansatz for the ground state ψ_0 and the excited state ψ_1 respectively. Fitting the equation for $\tilde{q_0}$ to the data, we find an effective interaction $\tilde{g} = (5.2 \pm 2.3) \times 10^{-5}$.

5.1 Results

Like discussed in section 2.1 measurements can be done because photons leak out of the micro cavity. These photons are captured on a CCD camera and from the color and intensity of the image one can determine how many particles are in a particular state. In figure 9 typical measurement are shown for **(a)** the ground state and **(b)** the excited state. Changing the rate of the pump laser gives different data points.

5.1.1 Effective interaction

Normally, the lengths q_0 and q_1 are measured in terms of the amount of pixels captured on the camera. Equations (27) and (28) for $\tilde{q_0}$ and $\tilde{q_1}$ however are scaled to the harmonic oscillator length l_{HO}. In figure 10a the experimental data of q_0 is plotted against the total number of particles $N = N_0 + N_1$. We only present the data of q_0 because the radius q_1 of the excited state has a large uncertainty. To scale q_0 to the harmonic oscillator length we note that for one particle in the ground state the length should be equal to l_{HO}. Therefore we extrapolated the first two data points linearly to one particle and took that length to scale our data with. We see clearly that for more particles in the condensate, the radius increases. This indicates a polarization $p \leq \frac{1}{3}$. And indeed, figure 10c shows even a polarization smaller then zero.

For every data point of figure 10a we have a matching polarization. By fitting every point to equation (29) we can determine $x = \tilde{g}N$ for these points. The results are plotted in figure 10b. We can divide every $\tilde{g}N$ by it's corresponding value of N which gives us values for $\tilde{g}$. All these values are of the order 10^{-5} and the average value gives us an estimate for the effective interaction of

$$\tilde{g} = (5.2 \pm 2.3) \times 10^{-5}. \tag{59}$$

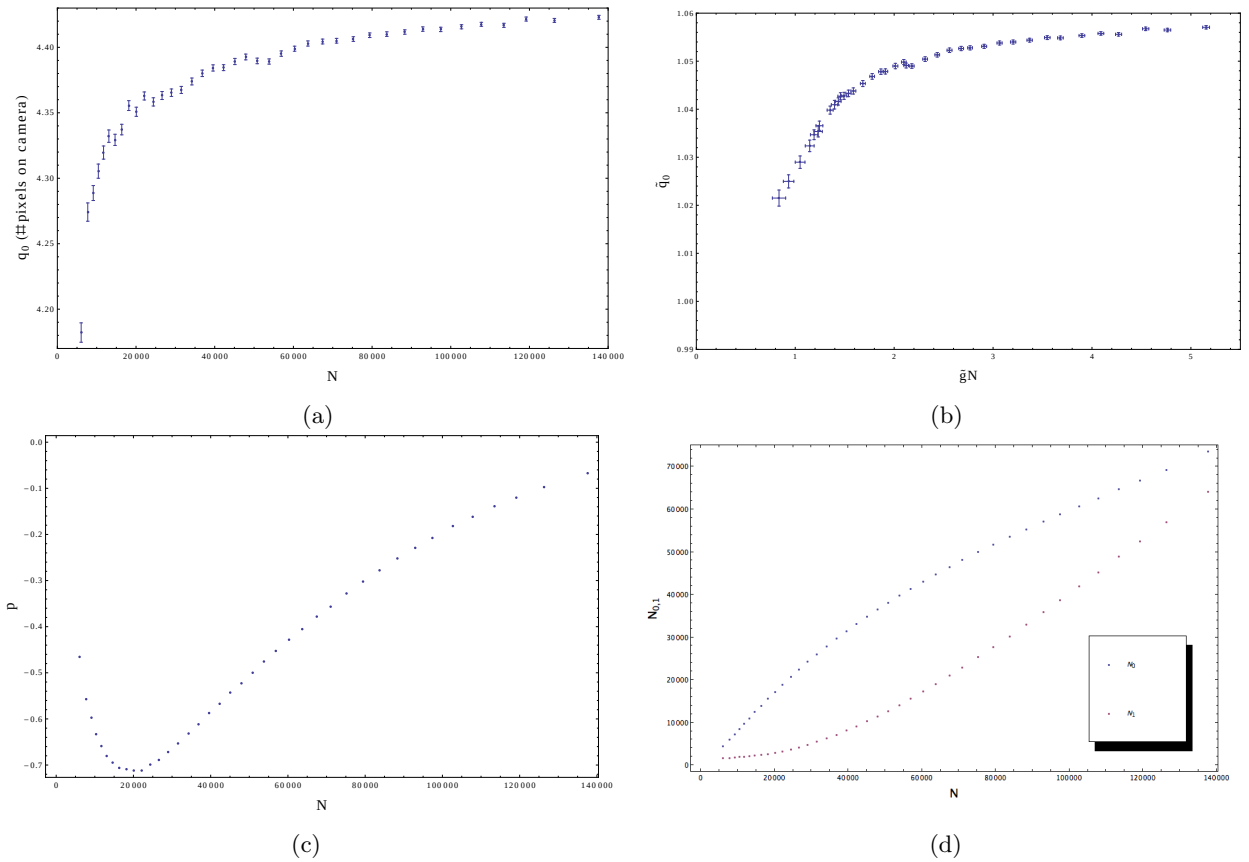

Figure 10: Plots of the experimental data. **(a)** The condensate radius q_0 of the ground state plotted against the total particles $N = N_0 + N_1$. Here, q_0 is measured in units of pixels captured on the camera. **(b)** Plot of $\tilde{q_0}$ against the fitted $\tilde{g}N$. **(c)** Figure of the polarization p against N. **(d)** The photon numbers N_0 and N_1 against N.

5.1.2 Photon numbers

In figure 10d, plots of the photon occupation numbers N_0 and N_1 are shown as a function of N. To obtain the experimental data, a large Gaussian pump spot was used of about 20 oscillator lengths. So, one of our approximations of the previous section is fulfilled. To see how well our other approximations are, we can try to fit the parameters of equation (47) to the data. From Keeling and Kirton [12] we set $\Gamma_\downarrow = 250 \times 10^6$. We know that for small pump rates, the photon numbers depend linear on this pump rate. This looks indeed satisfied for the first, say 10 data points for N_0 and N_1. If we expect that at low pump rate the photon occupation numbers are purely due to thermalization, we can obtain from the slope of these lines and equation (54) an estimate for the effective parameters $\alpha_m = \Gamma_\downarrow e^{\beta\delta_m}$. When we look at the curvature of the data points, we expect that the curve of N_0 is described by η_0 slightly above 1. However, for N_1 we expect η_1 slightly below 1. Varying these parameters we obtained

$$\alpha_0 = 7.5 * 10^9, \qquad \alpha_1 = 7.75 \times 10^{10}, \qquad \eta_0 = 1.00001, \qquad \eta_1 = 0.99992.$$

The result is plotted in figure 11 for both the photon occupation numbers and the polarization. For the ground state, figure 11a indicates the convergence to an asymptote. For the excited state, the phenomena of lasing can be seen.

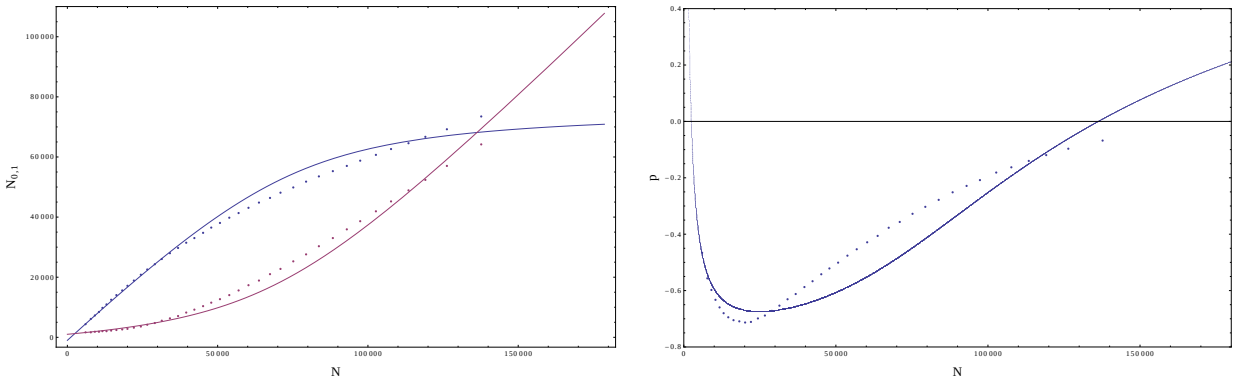

(a) (b)

Figure 11: Experimental data together with the first fits of the theoretical curves for the **(a)** photon numbers N_0 and N_1 and **(b)** the polarization as function of the total photon number N.

5.2 Discussion

The obtained dimensionless effective interaction is of the order $\tilde{g} \simeq 10^{-5}$. Let's first compare this with the results of Greveling et al. [4], which we discussed in section 2.4. The effective interaction they found was of the order $\tilde{g} \simeq 10^{-2}$, so at first sight it looks our effective interaction is much smaller. In Klaers et al. [6] they determined also an effective interaction by looking at the condensate radius of the ground state. They found $\tilde{g} = (7 \pm 3) \times 10^{-4}$ which is a factor 10 larger. This is what we expected beforehand, because we argued earlier that they measured a too large condensate radius. However, up to this point one has to handle the result carefully and shouldn't make quick conclusions. The number of photons that leak out of the cavity are a measure for the total number of photons in the states. So only N_0 and N_1 are relatively well defined to each other and this was the reason to define the polarization p. It has the result that the value of $\tilde{g}$ can differ a yet unknown factor. This factor can both increase and decrease $\tilde{g}$. So, only when we know this factor we can make a solid conclusion for our effective interaction. Calibration of the experimental set up is needed for N.

The way we found our solutions, with perturbation in $\tilde{g}N$, has as advantage that the values of $\tilde{g}N$ from figure 10b are well defined. This means that although we can't make a solid solution for $\tilde{g}$, we can conclude that the pattern shown in the figure indicates a reliable effective interaction.

We tried to fit our theoretical curves for the condensate numbers to the data. Although our results look far from perfect, our models gave solutions which indicates that we are in the right direction. So, we can still say a few relevant things about them. First of all, we found the expected strong dependence of the photon number on the parameter η_m. The estimated values don't seem to differ much, but their slightly modification of the critical value 1 gives very different result. Because $\eta_0 > 1$ we can conclude that for the ground state the cavity decay rate has slightly the upper hand with respect to the emission rates. Though, this effect seems small, it changes the photon number a lot and we expect for this state that the photon number will saturate. For the excited state we have $\eta_1 < 1$, so the cavity decay rate is slightly inferior to the emission rate. The effect is that we expect lasing for higher pump rates. However, it doesn't seem that we are near the threshold pump rate for which we expect this yet. Furthermore we note that the curves seem to fit for small N, but when N gets larger our curves don't fit well anymore. The excited state doesn't seem to grow as fast as we expect and the ground state doesn't seem to converge that well. A likewise effect is that the well in the polarization isn't that sharp as what follows from the data. This can either be due to the fact that our estimates for the fitted parameters need to be better. Or because for large pump rates our approximations from section 4.4 aren't valid anymore. Further research need to be taken before we can say more.

5.3 Conclusion

We have found an effective interaction $\tilde{g} = (5.2 \pm 2.3) \times 10^{-5}$ which is a factor 10^3 smaller then the results of Greveling et al. [4] discussed in section 2.4. Furthermore it is a factor 10 smaller then the results found in Klaers et al. [6]. This was what we expected beforehand because we have taken an extra excited state into account. However, one should interpret this result carefully. As discussed above, $\tilde{g}$ can differ a yet unknown factor. Calibration of the experimental set up for N is needed to exclude this factor and to make a solid conclusion. Nevertheless, the values of $\tilde{g}N$, shown in figure 10b, are well defined and can be used later on. Furthermore, figure 10b shows indeed a reliable interaction.

Our theoretical model for the photon occupation numbers gave a first insight in which effects are the important ones. From the fitted curves in figure 11 we see our models capture the right trend to explain the data. It led to the conclusion that cavity decay versus emission rates is very important in the behavior of the states. It can be the difference for which we expect lasing or saturation of the photon numbers. However, the curves are far from perfect and we expect that our models need to be improved before we can make better conclusions about the large pump rate behavior of the photon numbers.

Acknowledgements

I would like to thank my supervisor Henk Stoof for his help and support during my research project. Further, I would like to thank ITF for giving the ability of doing my project there. Finally I would like to thank Dries van Oosten and Charly Beulenkamp for their input and help on the experimental side of my project. They provided me with experimental data when necessary and we had some useful discussion of how I could implement the data in my theoretical models.

References

[1] A. Einstein, Sitz. ber. Preuss. Akad. Wiss. **1**, 3 (1925).

[2] J. Klaers, F. Vewinger, and M. Weitz, Nature Physics **6**, 512 (2010).

[3] J. Marelic and R. A. Nyman, Phys Rev. A **91**, 033813 (2015).

[4] S. Greveling, F. van der Laan, K. L. Perrier, and D. van Oosten, ArXiv e-prints (2017), 1712.07922.

[5] R. A. Nyman and B. T. Walker, Journal of Modern Optics **65**, 754 (2018).

[6] J. Klaers, J. Schmitt, F. Vewinger, and M. Weitz, Nature **468**, 545 (2010).

[7] J. Marelic, B. T. Walker, and R. A. Nyman, Phys. Rev. A **94**, 063812 (2016).

[8] E. van der Wurff, A.-W. de Leeuw, R. Duine, and H. Stoof, Phys. Rev. Lett. **113**, 135301 (2014).

[9] K. L. Perrier, Master's thesis, Utrecht University, Utrecht (2016).

[10] D. J. Griffiths, *Introduction to Quantum Mechanics* (Pearson, Edinburgh Gate, 2014), 2nd ed., ISBN 1-292-02408-9.

[11] N. W. Ashcroft and N. D. Mermin, *Solid State Physics* (CENGAGE Learning, Cornell University, 1976), 17th ed., ISBN 978-81-315-0052-1.

[12] J. Keeling and P. Kirton, Phys. Rev. A **93**, 013829 (2016).